# Lipid Profiling of *Synechococcus* sp. PCC7002 and Two Related Strains by HPLC Coupled to ESI-(Ion Trap)-MS/MS

Olimpio Montero

Centre for Biotechnology Development (CDB, CSIC), Francisco Vallés 8, 47151 Boecillo (Technological Park), Valladolid, Spain. Fax: +34 983 184800.
E-mail: olimpio.montero@dicyl.csic.es

Z. Naturforsch. **66c**, 149–158 (2011); received August 11/December 9, 2010

The lipid profiles of *Synechococcus* sp. PCC7002 and two related 16S rDNA (99% identity) strains were established by a new method of high-performance liquid chromatography coupled to electrospray-mass spectrometry (HPLC-MS). Lipids were analysed in the positive and negative ionization mode, and fragmentation patterns are reported. No differences in the lipid profile between the three strains could be observed, but the relative content of some species differed. Major lipid species were found to be 1-octadecatrienoyl-2-hexadecanoyl-3-(6'-sulfo-*α*-D-quinovosyl)-*sn*-glycerol [SQDG (18:3/16:0)] and 1-octadecatrienoyl-2-hexadecenoyl-3-*β*-D-monogalactosyl-*sn*-glycerol [MGDG (18:3/16:1)]. Ten species of SQDG, six species of PG (phosphatidyl-glycerol), seven species of MGDG, and two species of DGDG (digalactosyl-diacyl-glycerol) were detected. A PG species (*m/z* 761) containing hydroxylinolenic acid or oxophytodienoic acid acyl ester ($C_{18}H_{32}O_3$), and SQDG species containing C17:1 and C17:3 fatty acyl esters are reported for the first time in cyanobacteria. The method also allowed the separation of two pairs of closely related isobaric MGDG species (*m/z* 770 and *m/z* 772 in positive ionization).

*Key words: Synechococcus*, Glycerolipids, HPLC-(ESI)-MS/MS

## Introduction

In addition to carotenoids and chlorophyll *a* (Chl*a*), cyanobacterial lipids are mainly composed of glycolipids and phosphatidyl-glycerol (PG). The glycolipids encompass sulfoquinovosyl-diacyl-glycerol (SQDG), monogalactosyl-diacyl-glycerol (MGDG), and digalactosyl-diacyl-glycerol (DGDG) (Wada and Murata, 1998; Kim *et al.*, 1997, 1999; Hölzl and Dörmann, 2007; Sato and Wada, 2009). The role of PG and SQDG in photosynthesis function has been the subject of a number of studies using mutants defective in PG or SQDG biosynthesis, which have been reviewed by Sato (2004). In *Synechocystis* sp. PCC6803, depletion of PG is associated with repression of photosystem I (PSI) synthesis and reduced Chl*a* content, whereas SQDG seems to be primarily responsible for photosystem II (PSII) structural and functional integrity at the donor side; a PG species containing 3,4-*trans*-hexadecenoic acid (C16:1) was suggested to be necessary for LHCII protein assembly. Furthermore, a recent paper by Domonkos *et al.* (2009) suggests that depletion of PG could be involved in regulation of the carotenoid biosynthetic pathway, thus linking photosynthetic pigments and membrane lipid composition. Hence, a detailed description of the lipidome at species level is required to understand membrane structure changes owing to different physiological states.

Kim *et al.* (1997, 1999) used fast-atom bombardment (FAB) coupled to four-sector MS/MS to analyse the glycolipid composition of *Synechocystis* sp. PCC6803 by direct injection with prior purification using bidimensional thin-layer chromatography (2D-TLC). They obtained in this way a high content of the sodium adducts $[M+Na]^+$ and $[M'–H+2Na]^+$, where M is MGDG or DGDG, and M' is SQDG or PG, which ren-

*Abbreviations:* DGDG, digalactosyl-diacyl-glycerol; 2D-TLC, bidimensional thin-layer chromatography; ESI, electrospray ionization; FAB, fast-atom bombardment; HPLC-MS/MS, high-performance liquid chromatography coupled to tandem mass spectrometry; MGDG, monogalactosyl-diacyl-glycerol; MGlcDG, monoglucosyl-diacyl-glycerol; PG, phosphatidyl-glycerol; SQDG, sulfoquinovosyl-diacyl-glycerol; 16S rDNA, ribosomal DNA of the 16S subunit; TQMS, triple-quadrupole mass spectrometry.

0939–5075/2011/0300–0149 $ 06.00 

dered stable fragmentation patterns. SQDG and PG species could also be analysed by these authors in the negative mode obtaining the $[M–H]^-$ ion. A similar procedure was used by Welti *et al.* (2003) to show how the lipid profile of plant chloroplasts could be characterized by means of mass spectrometric measurements, but they used electrospray ionization (ESI) and triple-quadrupole mass spectrometry (TQMS). Characteristic collision-induced (CID) fragments were reported in the latter studies for MGDG and DGDG (*m/z* 243 in positive mode), SQDG (*m/z* 225 in negative mode), and PG (*m/z* 153 or *m/z* 227 in negative mode and high or low collision energy, respectively). No chromatographic separation was used in these cases. Balogi *et al.* (2005) used LC-MS analysis to confirm the presence of monoglucosyl-diacyl-glycerol (MGlcDG) in *Synechocystis* sp. PCC6803, but no detailed data on the different lipid species found were reported. And more recently, Okazaki *et al.* (2009) developed a method using LC-MS with the aim of determining enzymes involved in the first steps of sulfolipid biosynthesis in *Arabidopsis* leaves. Using a peak area-based relative quantification, main species determined by these authors were MGDG (34:6), PG (34:4), DGDG (36:6), and SQDG (34:3). Hence, according to these authors' results, MS has become an adequate tool for cyanobacterial and thylakoid lipid analysis.

Two *Synechococcus* strains from the Culture Collection of the Institute of Marine Sciences of Andalusia (ICMAN, CSIC), namely *Synechococcus* sp. 01/0201 (Syn01) and *Synechococcus* sp. 01/0202 (Syn02), were found to exhibit 99% identity to *Synechococcus* sp. PCC7002 with regard to 16S rDNA and 94% identity with regard to the *crtR* gene (Montero *et al.*, unpublished results). Even though the lipid composition of *Synechococcus* sp. PCC7002 was reported by Sakamoto *et al.* (1997), specific association of fatty acids with the different lipid species could not be established because the analysis was carried out by TLC with subsequent gas-liquid chromatography of methyl esters. Hence, using the advantage of ESI-MS/MS as it is implemented at present (Hsu and Turk, 2001; Sato, 2004), it was found of interest to determine the lipid profiles of these cyanobacterial strain at species level using a new HPLC-MS (high-performance liquid chromatography coupled to electrospray-mass spectrometry) method.

## Material and Methods

### *Cell cultures*

Cyanobacterial cells were grown in 100-mL Erlenmeyer flasks with 50 mL of culture volume, at 20 °C and an irradiance of 60–80 $\mu$mol $m^{-2}$ $s^{-1}$ from daylight fluorescent tubes. Nutrients were added as in the F/2 medium of Guillard and Ryther (1962) but with doubled nitrate concentration. Natural sea water, filtered through 1.0-$\mu$m glass fiber filters and autoclaved (120 °C, 1.1 kg $m^{-2}$ pressure), was used as culture medium for the *Synechococcus* sp. strains 01/0201 (Syn01) and 01/0202 (Syn02), from the Culture Collection of the Institute of Marine Sciences of Andalusia (ICMAN, CSIC, Cádiz, Spain). The same natural sea water, but diluted with distilled water to salinity 21‰ (salinity of natural sea water is 37‰) was used to culture *Synechococcus* sp. PCC7002. The *Synechococcus* sp. PCC7002 strain was obtained from the Pasteur Culture Collection (PCC) of Cyanobacteria (Paris, France) and was adapted to the culture medium used in these experiments for at least 6 growth cycles, with a growth period of 14–16 d each. Culture samples were always harvested for the different extraction protocols in the mid to late exponential growth phase (8–10 d of growth), from at least three independent cultures (five for *Synechococcus* sp. PCC7002).

### *Sample extraction*

Lipids were extracted from cell biomass of three to five independent cultures. A cell culture aliquot of 5 mL was centrifuged (2818 × *g*, 10 min, 4 °C), the supernatant discarded, and the pellet washed with 1 mL 9% aqueous NaCl solution. After a new centrifugation, 0.5 mL methanol was added to the pellet and sonicated for 1 min while the tube was immersed in ice. The supernatant was recovered after another centrifugation and kept in blue Eppendorf-like tubes at –20 °C until analysis.

### *HPLC-MS/MS*

For MS analysis, HPLC separation was carried out in a LaChrom Elite® HPLC system from VWR-Hitachi (VWR International Eurolab S.L., Barcelona, Spain), which consisted of an L-2130 binary pump equipped with a low-pressure gradient accessory and in-line degasser, an L-2420 UV-Vis detector, and an L-2200 autosampler. Samples

were analysed using a Nucleosil (Teknokroma, Barcelona, Spain) 120 C18 column (4.0 × 150 mm, 5 $\mu$m particle size) with an ODS guard column (4.6 × 10 mm, Teknokroma). A gradient elution was used for separation as follows: (1) initial 80% A + 20% B; (2) 5 min linear gradient to 15% A + 85% B; (3) 8 min isocratic; (4) 10 min linear gradient to 0% A + 100% B; (5) 16 min isocratic; (6) 20 min linear gradient to 80% A + 20% B; (7) 30 min linear gradient to 2% A + 98% C; (8) 50 min isocratic; (9) 60 min linear gradient to 80% A and 20% B; and (10) 75 min isocratic; where solvent A is methanol/acetonitrile/5 mM aqueous ammonium acetate (75:15:10), solvent B is acetonitrile/5 mM aqueous ammonium acetate (90:10), and solvent C is 100% methanol. The flow rate was 0.3 mL $min^{-1}$, and 50 $\mu$L were injected.

Column effluent was connected on-line to a UV detector (L-2420 from VWR-Hitachi), with detection set at 450 nm, and an ion-trap (IT) mass spectrometer Esquire® 6000 from Bruker Daltonics S. A. (Bremen, Germany), which was equipped with an ESI source. Compounds were simultaneously detected in the negative (ESI–) and positive (ESI+) ion mode in full scan. Mass spectrometer parameters for the analysis were: nebulizer, 45 psi; dry gas ($N_2$), 9.0 L $min^{-1}$; dry temperature, 320 °C; capillary current, ± 3500 V; scan, 50–1200 *m/z*; collision gas, helium. Data were afterwards analysed using the Data Analysis® software from Bruker Daltonics S. A. LC-MS/MS was further conducted for selected samples for identification of the different lipids.

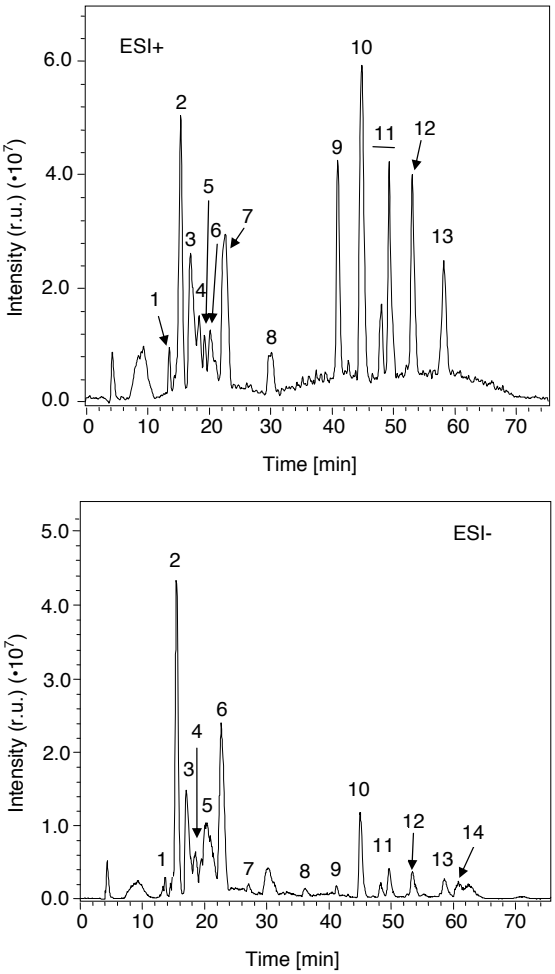


Fig. 1. Base peak chromatograms obtained in the HPLC-MS analysis of methanolic extracts with positive (ESI+) and negative (ESI–) ionization. Main *m/z* corresponding to each chromatographic peak are as follows (peak number, *m/z*): (ESI+): 1, 832; 2, 834; 3, 660, 741; 4, 836; 5, 313; 6, 762; 7, 838; 8, 359; 9, 930; 10, 768; 11, 770; 12, 772; 13, 774; (ESI–): 1, 813; 2, (741), 815; 3, 658, 791; 4, 817; 5, 743; 6, 819; 7, 745; 8, 747; 9, 911; 10, 809; 11, 811; 12, 813; 13, 815; 14, 981.

## Results

A base peak chromatogram (BPC) with well defined peaks was obtained for both positive (ESI+) and negative (ESI–) ionization for the three strains (Fig. 1). Since no differences in membrane lipid composition could be observed between the three strains, data shown in this study are representative of those obtained for the three strains, although they mostly refer to *Synechococcus* sp. PCC7002. Up to ten SQDG species, seven MGDG species, two DGDG species, and six PG species could be detected as shown in Tables I, II, and III. Two pairs of isobaric MGDG compounds (*m/z* 770 and *m/z* 772 in ESI+) could be clearly resolved with this method (peaks 11 and 12 in ESI+). Ionic species were detected as the ammonium adduct ion ($[M+NH_4]^+$) in the positive mode, whereas the deprotonated ion ($[M–H]^-$), and the chloride ($[M+Cl]^-$) and acetate ($[M+Ac]^-$) adduct ions, respectively, were detected in the negative mode. The averaged mass spectra obtained with negative ionization for the SQDGs and PGs that eluted between 12 and 34 min, on one hand, and for the MGDGs that eluted between 43 and 62 min, on the other hand, are shown in Figs. 2A and 3A, respectively. Three peak groups can be

Table I. Representative species of sulfoquinovosyl-diacyl-glycerol (SQDG) detected in methanolic extracts of *Synechococcus* sp. PCC7002 and two related *Synechococcus* strains (Syn01 and Syn02) by electrospray ionization-ion trap-mass spectrometry (ESI-IT-MS and ESI-IT-MS/MS).

| Species | *m/z* ESI– ($[M–H]^-$) | *m/z* ESI+ ($[M+NH_4]^+$) | (ESI–)-MS/MS fragments |
|---|---|---|---|
| SQDG (18:3/16:1) | 813.6 | 832.6 | 225, 253, 277, 535, 559 |
| SQDG (18:3/16:0) | 815.7 | 834.5 | 225, 255, 277, 537, 559 |
| SQDG (18:2/16:0) | 817.6 | 836.6 | 225, 255, 279, 537, 561 |
| SQDG (18:1/16:0) | 819.6 | 838.2 | 225, 255, 281, 537, 563 |
| SQDG (18:0/16:0) | 821.5 | 840.5 | 225, 255, 283, 537, 565 |
| SQDG (16:0/16:1) | 791.3 | 810.4 | 225, 253, 255, (535), 537 |
| SQDG (16:0/16:0) | 793.6 | N.D. | 225, 255, 537 |
| SQDG (17:1/16:0) | 805.4 | N.D. | 225, 255, 267, 537, 549 |
| SQDG (17:3/16:0) | 801.4 | N.D. | 225, 255, 263, 537, 545 |
| SQDG (16:1/16:1) | 789.5 | N.D. | Only detected in full scan |

N.D., not detected. Very low intensity peaks are indicated in brackets.

Table II. Representative species of monogalactosyl-diacyl-glycerol (MGDG) and digalactosyl-diacyl-glycerol (DGDG) detected in methanolic extracts of *Synechococcus* sp. PCC7002 and two related *Synechococcus* strains (Syn01 and Syn02) by electrospray ionization-ion trap-mass spectrometry (ESI-IT-MS and ESI-IT-MS/MS).

| Species | *m/z* ESI– ($[M–H]^-$, $[M+Cl]^-$, $[M+Ac]^-$) | *m/z* ESI+ ($[M+NH_4]^+$) | (ESI–)-MS/MS (and $MS^3$) fragments |
|---|---|---|---|
| MGDG (18:3/16:1) | 749.6, 785.6, 809.6 | 768.5 | $MS^2$ 809: 233, 253, 277, 489, 513, 749; $MS^3$ 809→749: 253, 277, 489, 513 |
| MGDG (18:2/16:1) | 751.6, 787.6, 811.6 | 770.5 | 811: 233, 253, 279, 489, 515, 751 |
| MGDG (18:3/16:0) | 751.6, 787.6, 811.6 | 770.5 | 811: 233, 255, 277, 491, 513, 751 |
| MGDG (18:1/16:1) | 753.6, 789.6, 813.6 | 772.5 | 813: 233, 253, 281, 489, 517, 753 |
| MGDG (18:2/16:0) | 753.6, 789.6, 813.6 | 772.5 | 813: 233, 255, 279, 491, 515, 753 |
| MGDG (18:1/16:0) | 755.6, 791.6, 815.6 | 774.5 | 815: 233, 255, 281, 491, 517, 755; 755: 255, 281, 491, 517, 695 |
| MGDG (18:1/18:1) | 781.5, 841.5 | N.D. | 841: 281, (295), 489, 517 |
| DGDG (18:3/16:1) | 911.6, 947.6, 971.6 | 930.6 | 253, 277, 379, 397, 633, 657 |
| DGDG (18:3/16:0) | 913.6, 949.6, 973.6 | 932.6 | 255, 277, 379, 397, 595, 635, 657 |

N.D., not detected. Very low intensity peaks are indicated in brackets.

Table III. Representative species of phosphatidyl-glycerol (PG) detected in methanolic extracts of *Synechococcus* sp. PCC7002 and two related *Synechococcus* strains (Syn01 and Syn02) by electrospray ionization-ion trap-mass spectrometry (ESI-IT-MS and ESI-IT-MS/MS).

| Species | *m/z* ESI– ($[M–H]^-$) | *m/z* ESI+ ($[M+NH_4]^+$) | (ESI–)-MS/MS fragments |
|---|---|---|---|
| PG (18:3/16:1) | 741.5 | N.D. | (227), 253, 277, 487, 505 |
| PG (18:3/16:0) | 743.5 | 762.4 | 227, 233, 255, 277, 465, 487, 505 |
| PG (18:2/16:0) | 745.5 | N.D. | 227, 255, 279, 465, 489, 507 |
| PG (18:1/16:0) | 747.5 | N.D. | (227), 255, 281, 491, 509 |
| PG (18:1/18:1) | 773.4 | N.D. | 227, 281, 417, 491, 509 |
| PG ($C_{18}H_{32}O_3$/16:0) | 761.4 | N.D. | 255, 295, 431, 505, 523, 568, 581 NL: 193, 256, (296), 466, 506 |

N.D., not detected. NL, neutral loss. Very low intensity peaks are indicated in brackets.

recognized in the case of MGDGs that correspond to the ($[M–H]^-$, $[M+Cl]^-$, and $[M+Ac]^-$ ions.

MS/MS fragmentation of predominant ions detected in ESI–, that is the $[M–H]^-$ ion for SQDG and PG (Figs. 2B and 4B, respectively), and the $[M+Ac]^-$ ion for MGDG (Fig. 3B) and DGDG, yielded the respective carboxy anions of the fatty acids at positions *sn*-1 and *sn*-2 of the glycerol backbone; the $[M–H]^-$ ion was also obtained as the major peak in the case of MGDG and DGDG. The main MS/MS fragments are depicted in Tables I, II, and III for SQDG, MGDG and DGDG, and PG, respectively. $MS^3$ experiments of the $[M–H]^-$ ion resulting from MS/MS ($MS^2$) fragmentation of the $[M+Ac]^-$ ion rendered the same peak pattern like the acetylated ion, but fatty acid carboxy anions were the most intense peaks in this case (Fig. 3C). The presence of *m/z* 225 in the MS/MS spectrum was used to clearly identify SQDG species in negative ionization (Fig. 2A). Likewise, the fragment with *m/z* 227 allowed identification of PG species, although some peaks being shown in the extracted ion chromatogram of *m/z* 227 from $MS^2$ experiments (Fig. 4A) had to be rejected as being PG species because the *m/z* of the parent ion did not match the molecular mass of any PG. The lysoglycerolipid arising from the loss of an acyl chain in MS/MS fragmentation of PGs and MGDGs (and DGDGs) could be clearly identified in the neutral loss spectrum (see insets in Figs. 3B and 4B). In contrast, the neutral loss spectrum of SQDG species gave the neutral fatty acids as predominant peaks (Fig. 2B).

The MS/MS fragmentation pattern in ESI+ of the SQDG (18:3/16:0), PG (18:3/16:0), and MGDG (18:3/16:1) species is depicted in Fig. 5. Major peaks could be observed that originate from the loss of the characteristic head group. Thus, in Fig. 5A, *m/z* 591 corresponds to the loss of the dehydrosulfoglycosyl anion (*m/z* 225 in ESI–), and so does *m/z* 573, due to the loss of the sulfoglycosyl anion (*m/z* 243) from SQDG (18:3/16:0) (Cedergren and Hollingsworth, 1994). In Fig. 5B, *m/z* 573 ($[M–171]^+$) derives from the loss of the glycerol phosphate anion ($[C_3H_7O_2OPO_3H]^-$) in PG (18:3/16:0) (Hsu and Turk, 2001); and in Fig. 5C, *m/z* 571 ($[M–179]^+$) and *m/z* 589 ($[M–179+18]^+$) result from the loss of the galactose head group and acquisition of a proton or ammonium ion, respectively, in MGDG (18:3/16:1). The *m/z* 243 fragment that has been pointed out as serving for MGDG species identification (Kim *et al.*, 1999; Welti *et al.*, 2003) was also observed though as a minor peak (Fig. 5C). The lysoglycerolipids resulting from the loss of the fatty acid acyl chains as neutral acids are represented by *m/z* 539 and *m/z* 561 in Fig. 5A, *m/z* 449 in Fig. 5B, and *m/z* 479 and *m/z* 515 in Fig. 5C.

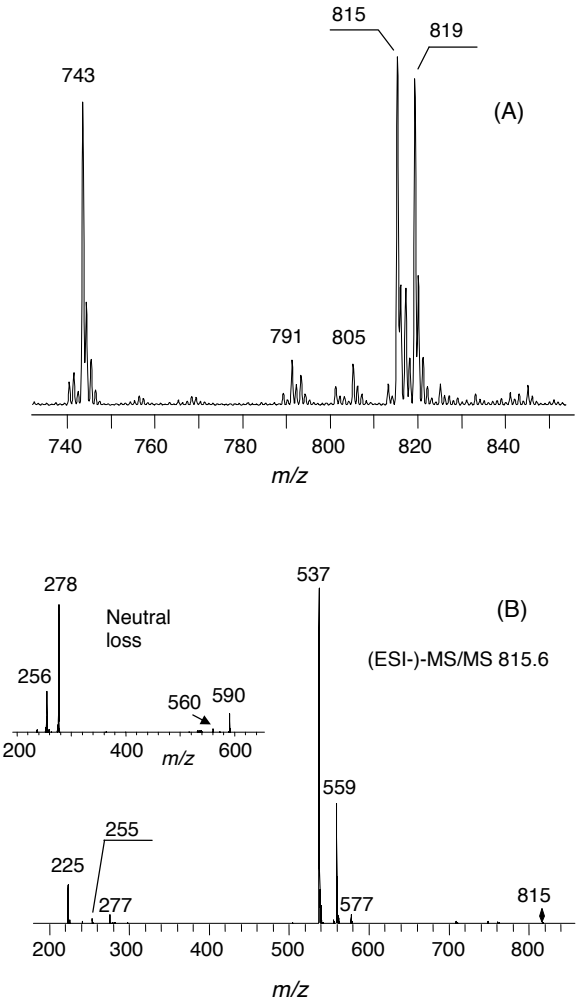


Fig. 2. (A) Averaged mass spectrum of the chromatographic region where the most abundant SQDG and PG elute (13–28 min). Numbers indicate the *m/z* of $[M–H]^-$ ions. (B) (ESI–)-MS/MS and neutral loss spectra of the parent ion ($[M–H]^-$) with *m/z* 815 [SQDG (18:3/16:0)]. Fragments: *m/z* 225 is the sulfoquinovosyl anion; *m/z* 255 is $[C16:0–H]^-$; *m/z* 277 is $[C18:3–H]^-$; *m/z* 537 is $[M–H–C18:3]^-$; *m/z* 559 is $[M–H–C16:0]^-$; *m/z* 577 is $[M–H–C16:0+H_2O]^-$; 560 is [M–C16:0]; 590 is [M–226].

Regarding the fatty acid composition, those species that combine C16:0 with C18:1, C18:2, and

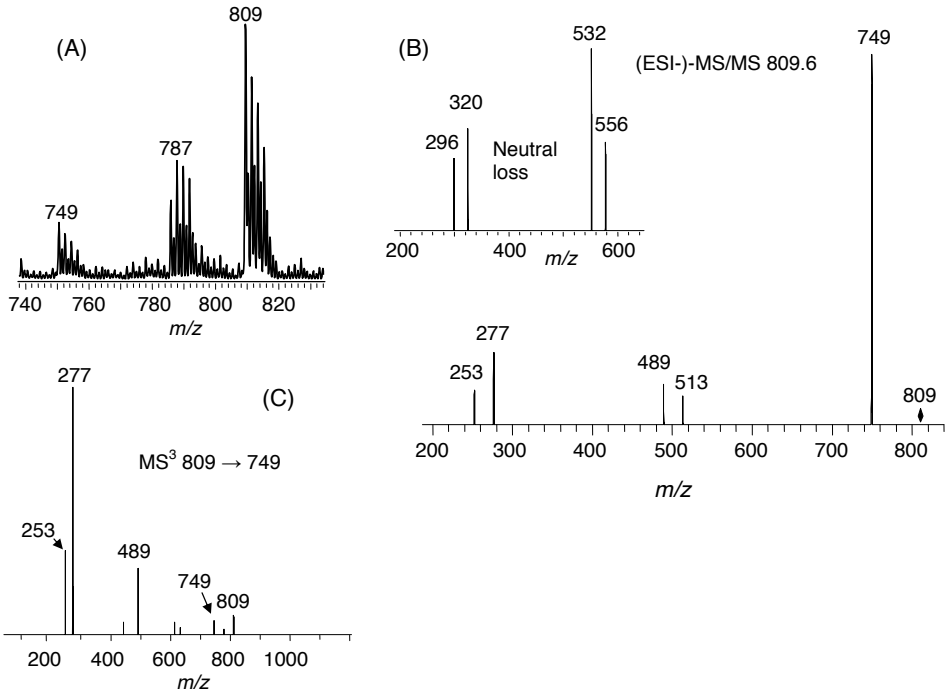


Fig. 3. (A) Averaged mass spectrum of the chromatographic region where the most abundant MGDG and DGDG elute (39–65 min). Numbers indicate the *m/z* of $[M–H]^-$, $[M+Cl]^-$, and $[M+Ac]^-$ ions of MGDG (18:3/16:1). (B) (ESI–)-MS/MS and neutral loss spectra of the parent ion with *m/z* 809 [MGDG (18:3/16:1)]. (C) $MS^3$ spectrum obtained for the transition *m/z* 809 → *m/z* 749 from MGDG (18:3/16:1). Fragments: *m/z* 253 is $[C16:1–H]^-$; *m/z* 277 is $[C18:3–H]^-$; *m/z* 489 is $[M–H–C18:3+H_2O]^-$; *m/z* 513 is $[M–H–C16:1+H_2O]^-$; *m/z* 749 is $[M–H]^-$; *m/z* 296 is $[C16:1–H+CH(CH_3)_2]$; *m/z* 320 is $[C18:3–H+CH(CH_3)_2]$; *m/z* 556 is [M–C16:1+AcH]; *m/z* 532 is [M–C18:3+AcH].

C18:3 were common to SQDG, MGDG, DGDG, and PG, but other species were specific for each glycerolipid class. In particular, only SQDG exhibited species in which hexadecenoic acid (C16:1) was combined with either itself or hexadecanoic acid (C16:0). Only two species of DGDG were detected, and both species had the C18:3 fatty acid (linolenic acid) combined with either hexadecanoic or hexadecenoic acids, respectively. An exclusive but minor species of PG was also observed in which hexadecanoic acid was combined with an acid yielding an ion of *m/z* 295, which according to LipidMaps search might be a derivative of hydroxylinoleic acid or oxophytodienoic acid (Table III), or otherwise it might also be a cyclopropyl-containing C18 fatty acid (Cedergren and Hollingsworth, 1994). Stearic acid (C18:0) was only found in SQDG species (Table I). Two species of SQDG were also detected that contained C17:1 and C17:3 fatty acids. The position of the acyl chains at *sn*-1 and *sn*-2 positions was determined from the relative abundance of the lyso species peaks following Kim *et al.* (1999), Guella *et al.* (2003), and Welti *et al.* (2003), or established according to data available in the literature (see below for a detailed discussion). Chlorophyll *a* was detected in ESI+ as the $[M+H]^+$ ion at *m/z* 893, while in ESI– it was detected as the $[M+Ac]^-$ adduct ion at *m/z* 951.

The relative content of the main species within every lipid class (*e.g.* SQDG, PG, and MGDG and DGDG), being represented by the corresponding *m/z* in the ESI– (A, B) or the ESI+ (C) spectrum, is compared in Fig. 6 for the three strains on a peak area basis, but normalized to the absorbance at 750 nm ($A_{750}$) and Chl*a* content of the cell suspension from which the methanol extract was obtained. SQDG (18:3/16:0), PG (18:3/16:0), DGDG (18:3/16:1), and MGDG (18:3/16:1) were the predominant lipid species in the three strains, with SQDG (18:1/16:0) and PG (18:3/16:1) showing a high content in *Synechococcus* PCC7002 as well. The content of all MGDG species exhibited the same order in Syn01 and Syn02 (Fig. 6C). PGs

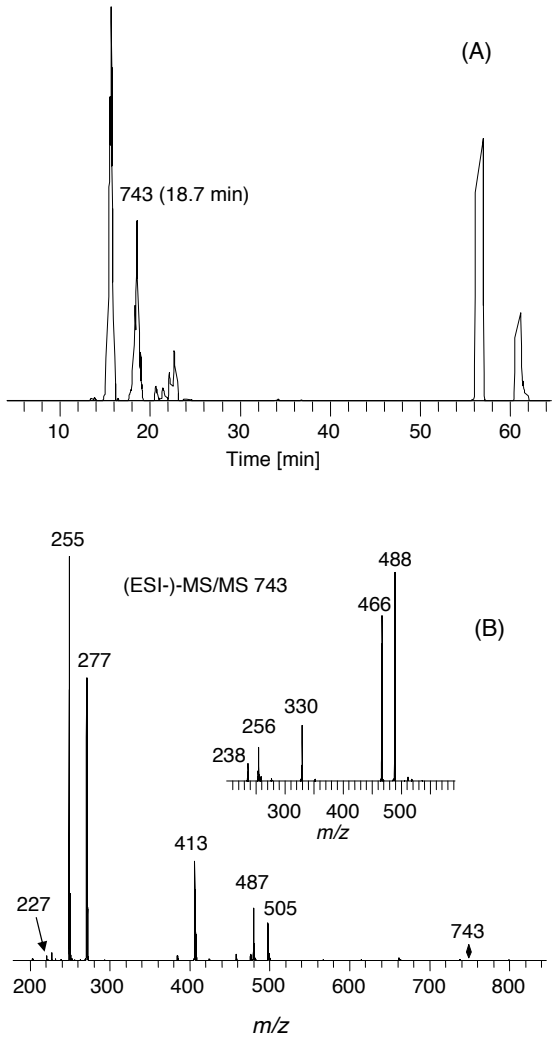


Fig. 4. (A) Extracted ion chromatogram of *m/z* 227 from MS/MS analysis. (B) MS/MS and neutral loss spectra of the parent ion ($[M–H]^-$) in negative mode (ESI–) with *m/z* 743 [PG (18:3/16:0)]. Fragments: *m/z* 227 is $[C_6H_{12}O_7P]^-$; *m/z* 255 is $[C16:0–H]^-$; *m/z* 277 is $[C18:3–H]^-$; *m/z* 487 is $[M–H–C16:0]^-$; *m/z* 505 is $[M–H–C16:0+H_2O]^-$; *m/z* 488 is [M–C16:0]; *m/z* 466 is [M–C18:3].

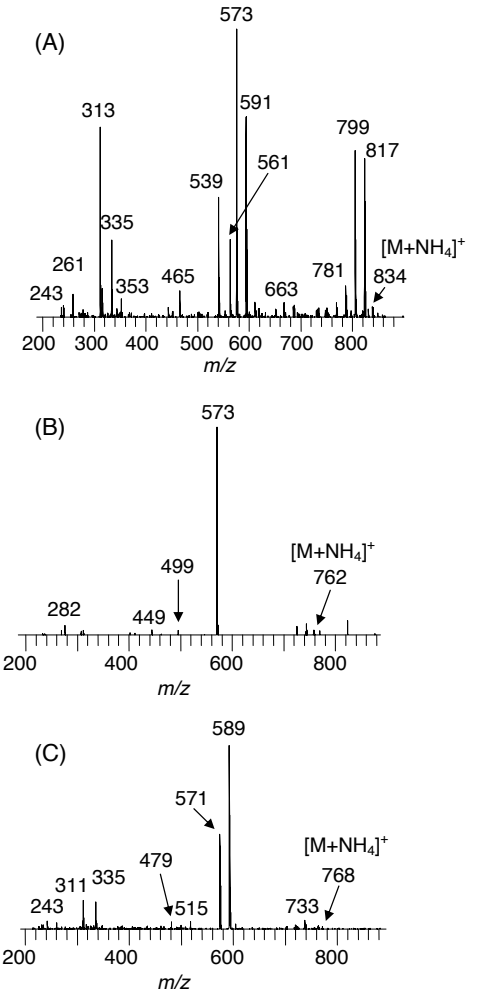


Fig. 5. MS/MS spectrum in the positive mode (ESI+) of (A) *m/z* 834 ($[M+NH_4]^+$) from SQDG (18:3/16:0); *m/z* 817 is $[M+H]^+$; *m/z* 573 is $[M–243]^+$, with *m/z* 243 corresponding to the sulfoquinovosyl anion; *m/z* 591 is $[M–225]^+$, with *m/z* 225 corresponding to the dehydrosulfoquinovosyl anion; *m/z* 539 and *m/z* 561 are $[M–RCO_2H+H]^-$ where RCOOH are the C18:3 and C16:0 fatty acids, respectively; (B) *m/z* 762 from PG (18:3/16:0); *m/z* 573 is $[M–171]^+$, with *m/z* 171 corresponding to the phosphoglycerol anion; *m/z* 449 is $[M–C18:3–H_2O+H]^+$; *m/z* 499 is $[M–227–H_2O]^+$; and (C) *m/z* 768 from MGDG (18:3/16:1); *m/z* 589 is [M–galactosyl+$NH_4$]$^+$ or [M–galactosyl+$H_2O$]$^+$; *m/z* 571 is [M–galactosyl]$^+$; *m/z* 479 is $[M–C16:1–H_2O–NH_4+H]^+$; *m/z* 515 is $[M–C16:1+NH_4+H]^+$; and *m/z* 243 is [galactosyl–$CH_2CH{=}CH_2$+Na]$^+$, where C18:3 and C16:0 are the neutral fatty acids.

amounted to 5–7% and were the least abundant lipid species, while MGDGs (44–45%) were the most abundant ones. DGDGs and SQDGs amounted to 10–17% and 32–40%, respectively.

## Discussion

The HPLC-MS analysis procedure used in this study provided a large set of glycerolipids that reflect the complex cyanobacterial membrane lipid composition (Kim *et al.*, 1999). The acyl groups of every lipid species could be clearly identified

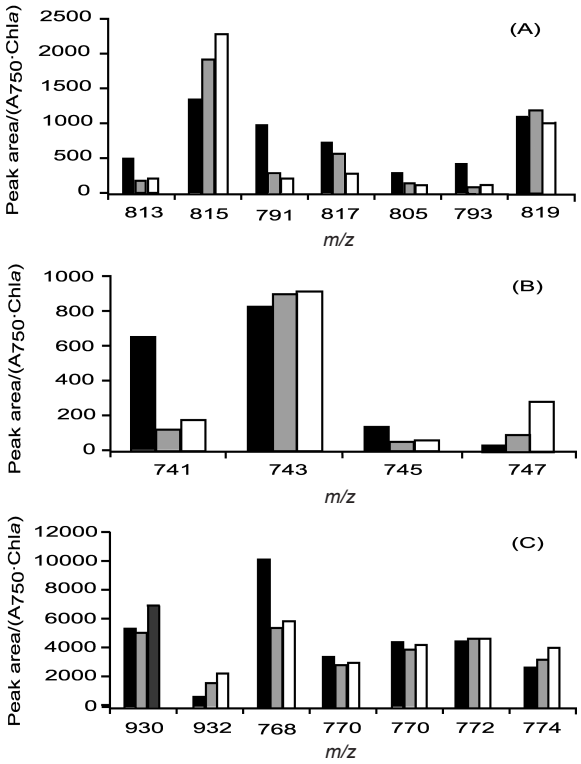


Fig. 6. Relative content, on a peak area basis, of the different species of (A) SQDG, (B) PG, both from ESI– chromatogram, and (C) DGDG and MGDG, from ESI+ chromatogram. The M, M+1 and M+2 were used for area calculation, where available. Chl*a* was determined from chromatographic pigment analysis. Black bars, *Synechococcus* sp. PCC7002; grey bars, Syn01; white bars, Syn02.

from the $[M–H]^-$ or $[M+Ac]^-$ ion fragmentation in the negative mode (Figs. 4B, 5B, and 6B), either from the MS/MS spectrum or the neutral loss spectrum. Furthermore, because $MS^3$ experiments are feasible in an ion-trap instrument, additional fragmentation could also be conducted where necessary (Fig. 3C). Specific *m/z* values resulting from the differential head group can serve the identification of each lipid class (Kim *et al.*, 1997, 1999; Welti *et al.*, 2003; Hsu and Turk, 2001). In the present study, the specific *m/z* value was clearly observed only for SQDG (*m/z* 225 in ESI–, Fig. 2B), whereas PG species (*m/z* 227 in ESI–, Fig. 4B) and MGDG species (*m/z* 243 in ESI+, Fig. 5C) yielded a peak with a very low intensity. Nonetheless, the extracted ion chromatogram (EIC) of the characteristic fragments could be drawn, as it is shown for *m/z* 227 in Fig. 4A, but further detailed analysis of the parent ion from each chromatographic peak is necessary because the specific *m/z* obtained in this way may also originate from other molecules; for example, *m/z* 227 serves to identify PG species (Hsu and Turk, 2001), but it may also be due to myristate (C14:0) (Takayama *et al.*, 1983). Therefore, analysis by direct injection might mislead lipid species determination, while this drawback can be overcome using HPLC separation, at least in ion-trap instruments (Balgoma *et al.*, 2010). MS/MS experiments in ESI+ did not give the typical acyl chain *m/z* because these are lost as the neutral ketenes or fatty acids. Nonetheless, these results may serve to underline (ESI–)-MS/MS-based compound identification, since major peaks reflect the cation resulting from the loss of the corresponding head group (see Fig. 5, legend), along with the lysoglycerolipids corresponding to the acyl chain lost, as for example *m/z* 539 and *m/z* 561 in Fig. 5A.

Regiospecifity of the acyl chain linkage to *sn*-1 or *sn*-2 positions of the glyceride backbone has been studied by different authors in SQDG, PG, MGDG, and DGDG species from cyanobacterial and thylakoidal membranes (Zepke *et al.*, 1978; Kim *et al.*, 1999; Hsu and Turk, 2001; Welti *et al.*, 2003; Guella *et al.*, 2003, and references cited therein). Their results have demonstrated that, in cyanobacterial membranes, C18 acyl chains are preferentially at the *sn*-1 position, while C16 acyl chains are at the *sn*-2 position. In (ESI–)-MS/MS (and $MS^3$) experiments, acyl chain regiospecificity can be ascertained in PG species from the relative abundance of the product ions resulting from the loss of each acyl chain (Hsu and Turk, 2001); thus, it has been shown that the product ion deriving from *sn*-2 acyl chain loss ($[M–R^2COO]^-$) is always more abundant than that deriving from *sn*-1 acyl chain loss ($[M–R^1COO]^-$). This fact is a consequence of fragmentation taking place through a charge remote-controlled mechanism, which makes losses from the *sn*-2 position sterically more favourable than losses from the *sn*-1 position. The same rule is applicable to the sodium adducts (ESI+) of galactolipid species in (FAB)-MS/MS experiments (Kim *et al.*, 1999), that is $[M–R^2COOH+Na]^+ > [M–R^1COOH+Na]^+$, where $R^x$ represents the acyl chain at the *sn-x* position, but opposite results ($[M–R^1COOH+Na]^+ > [M–R^2COOH+Na]^+$) are obtained when experiments are conducted in instruments with an ESI source

and ion-trap or TQ analysers (Guella *et al.*, 2003; Welti *et al.*, 2003). In this latter case, a possible dependence of the $[M–R^2COO]^-/[M–R^2COO]^-$ ratio upon collision energy in the fragmentation of negatively charged PG species with a C16 chain at the position *sn*-2 has been suggested by Welti *et al.* (2003). Our results are in agreement with the rule shown by Hsu and Turk (2001) for negatively charged PG species, since the peak at *m/z* 487 ($[M–2H–C16:0]^-$) is more abundant than the peak at *m/z* 465 ($[M–2H–C18:3]^-$) in the MS/MS spectrum, and *m/z* 488 is more intense than *m/z* 466 in the neutral loss spectrum (Fig. 4B). Moreover, the peak intensity of *m/z* 255 (palmitoyl chain) is higher than that of *m/z* 277 (linolenoyl chain). However, results opposite to these for PGs are illustrated in Figs. 2B and 3B for the SQDG and MGDG species, respectively. In the MS/MS spectrum of SQDG (18:3/16:0), the peak at *m/z* 537 that results from the C18:3 acyl chain loss is more intense than the peak at *m/z* 559 that results from the C16:0 acyl chain loss (Fig. 2B), and *m/z* 278 is more intense than *m/z* 256 in the neutral loss spectrum as well. Likewise, *m/z* 489 from C18:3 acyl chain loss is more intense than *m/z* 513 from C16:1 acyl chain loss in the fragmentation spectrum of MGDG (18:3/16:1) (Figs. 3B, C). Nonetheless, fragmentation results in ESI+ are contradictory. Thus, MGDG (18:3/16:1) rendered the lysoglycerolipids that correspond to the loss of C16:1, that is, *m/z* 479 and *m/z* 515, rather than the *m/z* corresponding to the loss of C18:3. Conversely, SQDG (18:3/16:0) gave also the fragment from the loss of the C18:3 acyl group in ESI+ as the most abundant peak, which is in agreement with the results of Guella *et al.* (2003) in relation to the fact that this fatty acid would esterify the *sn*-1 position of the glycerol backbone. Likewise, the presence of *m/z* 449, corresponding to the loss of the C18:3 acyl chain, in the MS/MS spectrum of PG (18:3/16:0) in ESI+ (Fig. 5B) would be in agreement with the results obtained for galactolipids, indicating that the C18:3 acyl chain would esterify the *sn*-1 position. Accordingly, taking into consideration that esterification of C16 fatty acids has been well established in different studies by diverse authors to be at the *sn*-2 position in membrane lipids of cyanobaceria, it is concluded that the fragmentation pattern of galactolipids is likely to occur through a different mechanism in ion-trap mass spectrometers operated in ESI– (and ESI+ for MGDGs as well), as compared to the charge remote one observed in triple-quadrupole and FAB mass spectrometers, at least under the conditions used in this study. Guella *et al.* (2003) suggested that charge remote and charge-driven mechanisms might operate simultaneously in an ion-trap instrument in MS/MS fragmentation through collision-induced dissociation (CID) under ESI–. Hence, further experimentation is necessary to unveil the underlying reasons for the aforementioned fragmentation differences to arise.

The predominant species in SQDG, and MGDG and DGDG contained octadecatrienoic acid (C18:3) along with either hexadecanoic (C16:0) or hexadecenoic (C16:1) acids, respectively. Recent work by Okazaki *et al.* (2006) pointed out that C16 fatty acids (either C16:0 or C16:1) esterified at the *sn*-2 position of glycerolipids are likely necessary for photosynthetic growth in *Synechocystis* sp. PCC6803, although the underlying reason still remains unknown. A PG species which is presumed to contain hydroxylinolenic acid (or another fatty acid derivative yielding *m/z* 295 in ESI–), as well as SQDG species containing a C17:1 (*m/z* 267) or a C17:3 (*m/z* 263) acyl group are reported for the first time in this study.

Despite the ionization rate in either ESI+ or ESI– is different from one lipid class to another (thereby, quantification is not feasible without appropriate standards), values calculated in the present study are almost identical with those reported by other authors (Sakamoto *et al.*, 1997; Kim *et al.*, 1999; Sato and Wada, 2009), although with SQDG being likely overrated.

In summary, a suitable HPLC-MS method is presented in this study for detailed analysis of membrane lipids in cyanobacteria and thylakoids. Further research is necessary to determine the mechanisms involved in the fragmentation process of MGDG, DGDG, and SQDG in ion-trap mass spectrometers.

*Acknowledgements*

Financial support from the Spanish Ministry of Education and Science (project reference AGL2004-08215-C03-02) is greatly appreciated. Thanks are given to A. Sánchez-Guijo for assistance in MS analysis.

Balgoma D., Montero O., Balboa M. A., and Balsinde J. (2010), Lipidomic approaches to the study of phospholipase $A_2$-regulated phospholipid fatty acid incorporation and remodeling. Biochimie **92**, 645–650.

Balogi Z., Török Z., Balogh G., Jósvay K., Shigapova N., Vierling E., Vígh L., and Horváth I. (2005), "Heat shock lipid" in cyanobacteria during heat/light acclimation. Arch. Biochem. Biophys. **436**, 346–354.

Cedergren R. A. and Hollingsworth R. I. (1994), Occurrence of sulfoquinovosyl diacylglycerol in some members of the family Rhizobiaceae. J. Lipid Res. **35**, 1452–1461.

Domonkos I., Malec P., Laczko-Dobos H., Sozer O., Klodawska K., Wada H., Strzalka K., and Gombos Z. (2009), Phosphatidylglycerol depletion induces an increase in myxoxanthophyll biosynthetic activity in *Synechocystis* PCC6803 cells. Plant Cell Physiol. **50**, 374–382.

Guella G., Frassanito R., and Mancini I. (2003), A new solution for an old problem: the regiochemical distribution of the acyl chains in galactolipids can be established by electrospray ionization tandem mass spectrometry. Rapid Commun. Mass Spectrom. **17**, 1982–1994.

Guillard R. R. L. and Ryther J. H. (1962), Studies on marine planktonic diatoms. I. *Cyclotella nana* Hustedt and *Denotula confervaceae* (Cleve) Gran. Can J. Microbiol. **8**, 229–239.

Hölzl G. and Dörmann P. (2007), Structure and function of glycoglycerolipids in plants and bacteria. Prog. Lipid Res. **46**, 225–243.

Hsu F.-F. and Turk J. (2001), Studies on phosphatidylglycerol with triple quadrupole tandem mass spectrometry with electrospray ionization: fragmentation processes and structural characterization. J. Am. Soc. Mass Spectrom. **12**, 1036–1043.

Kim Y. H., Yoo J. S., and Kim M. S. (1997), Structural characterization of sulfoquinovosyl, monogalactosyl and digalactosyl diacylglycerols by FAB-CID-MS/MS. J. Mass Spectrom. **32**, 968–977.

Kim Y. H., Choi J.-S., Yoo J. S., Park Y.-M., and Kim M. S. (1999), Structural identification of glycerolipid molecular species isolated from cyanobacterium *Synechocystis* sp. PCC 6803 using fast atom bombardment tandem mass spectrometry. Anal. Biochem. **267**, 260–270.

Okazaki K., Sato N., Tsuji N., Tsuzuki M., and Nishida I. (2006), The significance of C16 fatty acids in the *sn*-2 positions of glycerolipids in the photosynthetic growth of *Synechocystis* sp. PCC6803. Plant Physiol. **141**, 546–556.

Okazaki Y., Shimojima M., Sawada Y., Toyooka K., Narisawa T., Mochida K., Tanaka H., Matsuda F., Hirai A., Hirai M. Y., Ohta H., and Saito K. (2009), A chloroplastic UDP-glucose pyrophosphorylase from *Arabidopsis* is the committed enzyme for the first step of sulfolipid biosynthesis. Plant Cell **21**, 892–909.

Sakamoto T., Higashi S., Wada H., Murata N., and Bryant D. A. (1997), Low-temperature-induced desaturation of fatty acids and expression of desaturase genes in the cyanobacterium *Synechococcus* sp. PCC 7002. FEMS Microbiol. Lett. **152**, 313–320.

Sato N. (2004), Roles of the acidic lipids sulfoquinovosyl diacylglycerol and phosphatidylglycerol in photosynthesis: their specificity and evolution. J. Plant Res. **117**, 495–505.

Sato N. and Wada H. (2009), Lipid biosynthesis and its regulation in cyanobacteria. In: Lipids in Photosynthesis: Essential and Regulatory Functions, Advances in Photosynthesis and Respiration Series, Vol. 30 (Wada W. and Murata N., eds.). Springer Science + Business Media BV, Dainferu, South Africa, pp. 157–177.

Takayama K., Qureshi N., Mascagni P., Anderson L., and Raetz C. R. H. (1983), Glucosamine-derived phospholipids in *Escherichia coli*. J. Biol. Chem. **258**, 14245–14252.

Wada H. and Murata N. (1998), Membrane lipids in cyanobacteria. In: Lipids in Photosynthesis (Siegenthaler P.-A. and Murata N., eds.). Kluwer Academic Publishers, Dordrecht, The Netherlands, pp. 65–81.

Welti R., Wang X., and Williams T. D. (2003), Electrospray ionization tandem mass spectrometry scan modes for plant chloroplast lipids. Anal. Biochem. **314**, 149–152.

Zepke H. D., Heinz E., Radunz A., Linscheid M., and Pesch R. (1978), Combination and positional distribution of fatty acids in lipids from blue-green algae. Arch. Microbiol. **119**, 157–162.